Two Distinct Pathways Mediated by PA28 and hsp90 in Major Histocompatibility Complex Class I Antigen Processing

Taketoshi Yamano,[1] Shigeo Murata,[2] Naoki Shimbara,[3] Noriaki Tanaka,[4] Tomoki Chiba,[2] Keiji Tanaka,[2] Katsuyuki Yui,[1] and Heiichiro Udono[1]

[1]*Department of Molecular Medicine, Division of Immunology, Nagasaki University School of Medicine, Nagasaki 852-8523, Japan*

[2]*Department of Molecular Oncology, Tokyo Metropolitan Institute of Medical Science, and CREST, Japan Science and Technology Corporation, Tokyo 113-8613, Japan*

[3]*UpScience, Incorporated, Yokohama 244-8588, Japan*

[4]*First Department of Surgery, Okayama University Medical School, Okayama 700, Japan*

Abstract

Major histocompatibility complex (MHC) class I ligands are mainly produced by the proteasome. Herein, we show that the processing of antigens is regulated by two distinct pathways, one requiring PA28 and the other hsp90. Both hsp90 and PA28 enhanced the antigen processing of ovalbumin (OVA). Geldanamycin, an inhibitor of hsp90, almost completely suppressed OVA antigen presentation in PA28$\alpha^{-/-}/\beta^{-/-}$ lipopolysaccharide blasts, but not in wild-type cells, indicating that hsp90 compensates for the loss of PA28 and is essential in the PA28-independent pathway. In contrast, treatment of cells with interferon (IFN)-γ, which induces PA28 expression, abrogated the requirement of hsp90, suggesting that IFN-γ enhances the PA28-dependent pathway, whereas it diminishes hsp90-dependent pathway. Importantly, IFN-γ did not induce MHC class I expressions in PA28-deficient cells, indicating a prominent role for PA28 in IFN-γ–stimulated peptide supply. Thus, these two pathways operate either redundantly or specifically, depending on antigen species and cell type.

Key words: antigen presentation • cytotoxic T lymphocytes • immunity active • macrophage activation • transplantation immunology

Introduction

Intracellular or endogenous antigens are processed by the proteasome, generating MHC class I ligands (equivalent to CTL epitopes) recognized by $CD8^+$T cells (1–3). The 20S proteasome consists of two outer α-rings and two inner β-rings, stacked in the order of αββα. Both rings comprise seven α- or β-subunits. Substrate proteins are thought to go through the α-ring of the proteasome in order to reach the internal β-ring cavity where the catalytic sites are located. As the pore of the α-ring is very narrow or almost closed, substrate access is usually prevented (4), and thus the 20S proteasome by itself cannot generate peptides efficiently. To operate active proteolysis, the enzyme needs to associate with regulatory complexes to allow proteins or peptides to access the catalytic sections.

To date, two types of regulatory complexes have been identified in the cell. One is the 19S regulatory complex (also called PA700), comprising multiple subunits including six ATPases, which binds to the 20S proteasome to form the 26S proteasome capable of degrading ubiquitinated proteins in an ATP-dependent manner (5). The other is PA28 or the 11S regulator (REG) that greatly stimulates the peptidase activity of the 20S proteasome but does not assist the degradation of large proteins, even if they have already been ubiquitinated (6). PA28 is composed of two homologous subunits, PA28α and PA28β.

These two subunits assemble into a heterohexamer (α3β3) with alternating α and β subunits (7), or a heteroheptamer (α3β4 or a mixture of α3β4 and α4β3) (8) with a mass of ∼200 kD. PA28 is known to be directly associated with the 20S proteasome, forming the 'football-shaped proteasome' in which PA28 is attached to both ends of the central 20S proteasome or the 'hybrid proteasome' comprising the 20S proteasome armed by PA28 on one side and PA700 on the other (2, 9).

Address correspondence to Heiichiro Udono, Department of Molecular Medicine, Division of Immunology, Nagasaki University School of Medicine, Nagasaki 852-8523, Japan. Phone: 81-95-849-7071; Fax: 81-95-849-7073; E-mail: udonoh@net.nagasaki-u.ac.jp

Evidence indicates that PA28 accelerates the in vitro processing of MHC class I ligands from their polypeptide precursors by the 20S proteasome in a coordinated dual-cleavage manner (10, 11). In vivo analysis has shown also that overexpression of PA28α subunit enhances the processing of some viral epitopes in cells (12). Moreover, it was reported that mice deficient in the PA28β gene have defective production of CTLs after viral infection, probably due to impaired assembly of the 'immunoproteasome' (13), a modified version of the 20S proteasome whose three constitutively expressed β-type subunits (X/MB1, Y/delta, and Z) are replaced by IFN-γ–inducible subunits (low-molecular weight polypeptide [LMP]7, LMP2, and multicatalytic endopeptidase complex-like [MECL]-1, respectively) (2, 14).

These findings indicate that PA28 plays an important role in the processing of MHC I class ligands. In contrast, we recently showed that induction of the immunoproteasome by IFN-γ is not impaired in PA28$\alpha^{-/-}/\beta^{-/-}$ cells and that specific CTLs are normally generated against $OVA_{257–264}$ epitope, and influenza virus A (PR-8) derived K^b- and D^b-restricted NS2 and NP antigen peptides in these knockout mice, whereas processing of an epitope derived from a tumor antigen of murine B16 melanoma, tyrosinase-related protein (TRP2)*$_{181–188}$ is entirely dependent on PA28 (15). These observations suggest that PA28αβ is not a prerequisite for antigen processing in general, but plays an essential role in the processing of certain antigens. Hence, it is likely that there exists a compensatory system(s) for PA28 function in the processing of antigens, but the entity remains unknown so far.

The molecular chaperone hsp90 is one of the most abundant proteins in eukaryotic cells, comprising 1–2% of total cellular proteins even in conditions of nonstress. Hsp90 is an evolutionarily conserved protein and contributes to a wide variety of fundamentally common and species-specific processes in cells (16–18). For example, it is essential for maintenance of functional integrity of various fragile proteins, such as steroid hormone receptors and many of protein kinases (18).

It is also notable that hsp90 functions as a protein-folding machinery collaborating with other chaperone molecules, such as Hsp70 and hsp40, and cochaperones containing p23 and Hop (16, 17). Indeed, Hsp90 can bind nonnative proteins through N- and COOH-terminal domains for refolding (17). In addition, hsp90 appears to be closely linked to the protein degradation in the cell. In fact, hsp90 directly associates with the 20S proteasome, and thus can influence the enzyme activity (19, 20). Recent studies have also shown that hsp90 links misfolded proteins of aberrant structures to the ubiquitination pathway for selective elimination (21). It is noteworthy that the COOH-terminal domain is involved in binding the antigenic octapeptide of vesicular stomatitis virus G protein (22).

Evidence also suggests that hsp90 binds to tumor-associated MHC class I ligands or their precursors (23). The latter part of these observations strongly suggests that hsp90 might be involved in MHC class I antigen presentation, but the molecular basis of such role is still unclear. Using x-ray crystallographic analysis, Prodromou et al. (24) indicated that hsp90 comprises a deep pocket containing binding sites for geldanamycin (GA), an anti-cancer agent, as well as ATP/ADP at the NH_2-terminal region. Therefore, the ATPase and hence chaperone activity of hsp90 is inhibited by ansamycin drugs such as GA or herbimycin A (HA), indicating that GA and HA could serve as hsp90-specific inhibitors (25).

Here, we examined the roles of PA28 and hsp90 in the MHC class I–restricted antigen processing using GA and HA (inhibitors of hsp90) and cells derived from mice lacking PA28α and PA28β. We show that both PA28 and hsp90 accelerate the processing of C- but not NH_2-terminal flanking regions of MHC class I ligands.

Importantly, the results showed that hsp90 is essential for compensating the loss of PA28 function in LPS blasts of PA28$\alpha^{-/-}/\beta^{-/-}$ mice, resulting in nearly normal antigen presentation of $OVA_{257–264}$. In addition, we show that IFN-γ–induced up-regulation of MHC class I is defective in PA28$\alpha^{-/-}/\beta^{-/-}$ macrophages and dendritic cells. Our data provide novel insights into the roles of PA28 and hsp90 in MHC class I antigen processing.

Materials and Methods

Reagents, Proteins, and Peptides. Hsp90, hsc70, and gp96 were purified from ascitic fluid from mice injected with RL♂1 cells as described previously (23). cDNA of murine PA28α was amplified by reverse transcription (RT)-PCR from the mRNA of EL4 cells and cloned into 5′ BamHI and 3′ KpnI sites of the pQE31 expression vector (QIAGEN). The protein expression was induced in *Escherichia coli* strain M15 and purified as described previously (26). The $OVA_{257–269}$ (SIINFEKLTEWTS), $OVA_{248–264}$ (EVSGLEQLESIINFEKL), and $OVA_{248–269}$ (EVSGLEQLESIINFEKLTEWTS) peptides were synthesized by standard solid phase methods using F-mock chemistry in a peptide synthesizer (AMS422; Applied Biosystems) and purified by reversed-phase HPLC on a C8 column. $TRP2_{181–193}$ (VYDFFVWLHYYSV) was purchased from SAWADY Technology Co. GA was purchased from Sigma-Aldrich. HA was provided by Dr. Y. Uehara, the National Institute of Infectious Diseases, Tokyo, Japan.

Cells and Culture. E.G7 is an OVA cDNA transfected EL4 line (27). $OVA_{257–264}$ and $TRP2_{181–188}$ specific CTLs were induced from spleen cells of mice immunized with these peptides fused to hsc70 as described previously (26) and maintained by weekly stimulation with E.G7 and B16 melanoma cells, respectively, in the presence of syngeneic feeder cells and IL-2. LPS blasts and murine embryonic fibroblasts (MEFs) were prepared from PA28$\alpha^{+/+}/\beta^{+/+}$ and PA28$\alpha^{-/-}/\beta^{-/-}$ mice, as described previously (15).

Preparation of Retroviral Gene Transfer System. Mini-genes encoding $OVA_{257–269}$, $OVA_{248–264}$, and $OVA_{248–269}$ were cloned into pMSCVhyg (CLONTECH Laboratories, Inc.). PT67 pack-

*Abbreviations used in this paper: BFA, brefeldin A; ER, endoplasmic reticulum; GA, geldanamycin; HA, herbimycin A; LC, lactacystin; MEF, murine embryonic fibroblast; TAP, transporter associated with antigen processing; TRP, tyrosinase-related protein.

aging cells were transfected with 10 μg of these constructs by DOTAP Liposomal Transfection Reagent (Boehringer). The cells were selected by 300 μg/ml hygromycin for one week to obtain stable virus-producing cell lines. The virus titers were 1–3 × 10^7 CFU/ml for OVA mini-genes, as evaluated by culture with NIH3T3 cells. These supernatants were used for transfection analysis. cDNA of human hsp90 was obtained by RT-PCR from mRNA of peripheral blood mononuclear cells. For transfection of genes of PA28α or hsp90, cDNAs were cloned into 5′ HpaI and 3′ EcoRI sites for PA28α and XhoI site for hsp90 of pMSCV-puro. (CLONTECH Laboratories, Inc.) and virus producing PT67 cells were selected by 2 μg/ml puromycin. E.G7 cells were transfected by these retrovirus vectors and stable cell lines expressing the molecules were established as E.G7 PA28α and E.G7 hsp90 and E.G7 mock cells, then maintained in the presence of 5 μg/ml puromycin.

Loading of Peptides by Osmotic Shock or Retrovirus Infection and Antigen Presentation Assay. Osmotic introduction of peptides or proteins into EL4 cells was performed as described previously (26). Briefly, 2 × 10^6 pelleted cells were suspended in 200 μl warm (37°C) hypertonic buffer (0.5 M sucrose in 10% wt/vol polyethylene glycol 1,000 in RPMI) with or without synthetic peptides and 100 μg of hsp90, hsc70, gp96, or recombinant PA28α, and incubated for 10 min. Then, 15 ml of warm hypotonic buffer (RPMI 1640/dH_2O: 60%) was added immediately followed by a 2-min incubation. After centrifugation, the cells were washed twice and further incubated in the presence or absence of GA (5 μM), HA (5 μM), or lactacystin (LC; 50 μM) in serum-free RPMI for 3 h at 37°C, under 5% CO_2. For retroviral expression of OVA peptides, 5 × 10^5 EL4 cells were transfected for 3 h by retrovirus vector encompassing mini-genes encoding $OVA_{257–269}$, $OVA_{248–264}$, and $OVA_{248–269}$ at the doses indicated in the figure legends, and then the virus was washed off. These cells were labeled by 3.7 MBq $Na_2{}^{51}CrO_4$ (NEN Life Science Products) and used for standard ^{51}Cr-release assay. The CTL assay was performed in the presence of brefeldin A (BFA) to block the egress of newly assembled MHC class I molecules from the endoplasmic reticulum to the cell surface. In all cases, control cultures were incubated in DMSO at a concentration equivalent to those in the inhibitor preparations.

Western Blot Analysis. After disruption of the cells by sonication and centrifugation at 100,000 *g* for 1 h, the resulting supernatant and precipitate were used as the cytosol and membranous fractions, respectively. The resultant total materials were dissolved with sample buffer for SDS-PAGE and run on a SDS-PAGE gel, blotted onto a PVDF membrane, and probed with anti-hsp90 mAb (rat IgG, SPA-835, clone 16F1; StressGen Biotechnologies), anti-β_2 microglobulin (M-20: affinity purified goat polyclonal antibody; Santa Cruz Biotechnology, Inc.), anti-hsp70 mAb (rat IgG, SPA-815, clone 1B5; StressGen Biotechnology) and anti-grp94 (gp96) mAb (rat IgG, SPA850; StressGen Biotechnology), and anti-PA28α, β rabbit polyclonal antibodies (15). Biotin-conjugated goat anti–rat Ig(Fc) or rabbit IgG (H+L) was used as secondary Ab (Jackson ImmunoResearch Laboratories) and peroxidase-conjugated avidin was used for visualization. The quantity of each protein was assessed by densitometric analysis of ECL-exposed films. Polyclonal antibodies against PA28α and PA28β and transporter associated with antigen processing (TAP)2 were produced as serum from rabbits immunized with synthetic peptides, human $PA28\alpha_{22–37}$ (CTKTENLLGSYFDKKI) and $PA28\beta_{3–18}$ (KPCGVRLSGEARKQVE) and human $TAP2_{688–703}$ (CCQEGQDLYSRLVQQRLMD), respectively, and purified with peptide bound affinity columns.

RT-PCR. RT-PCR was used for quantification of transcripts of K^b and its control glyceraldehyde-3-phosphate dehydrogenase (G3PDH). For the amplification of K^b transcript, forward primer CCGAATTCATGGTACCGTGCACGCTGC and reverse primer CCTCTAGATCACGCTAGAGAATGAGG were used. For the amplification of G3PDH, ACCACAGTCCATGCCATCAC and TCCACCACCCTGTTGCTGTA for forward and reverse primers were used.

Flow Cytometric Analysis. Cells were incubated for 30 min with ascites obtained from 25.D1–16 hybridoma (murine IgG1, specific for K^b-$OVA_{257–264}$ [28], a gift from Dr. R. Germain, National Institutes of Health, Bethesda, MD) at 4°C, then washed twice followed by staining with FITC-conjugated rabbit anti–mouse IgG (H+L; Jackson ImmunoResearch Laboratories) for 30 min at 4°C. For staining of K^b molecules, biotin-conjugated anti–mouse K^b mAb derived from CTKb (Cedarlane Laboratories) and FITC-conjugated streptavidin (Jackson ImmunoResearch Laboratories) were used. For staining of LFA-1, M17/4.2 (rat IgG2a) and FITC-conjugated mouse anti–rat Ig(H+L) were used. The acid wash recovery assay was performed, as described previously (29). Briefly, cells were treated for 1.5 min with acid (1:1 mixture of 0.263 M citric acid and 0.132 M NaH_2PO_4 at pH 3.0), neutralized to pH 7.5 by adding 1 ml of 0.15 M NaH_2PO_4 and washed twice with PBS. The treated cells were further incubated for 3 h with GA or $OVA_{257–264}$ in the presence or absence of IFN-γ before FACS® analysis. Flow cytometric analysis was performed with FACScan™ (Becton Dickinson), and the data were analyzed by CELLQuest™ (Becton Dickinson). The experiments with FACScan™ were performed several times and results of one representative experiment are shown. The relative fluorescence was calculated after subtraction of the fluorescence of control (staining with only second antibody or FITC-conjugated streptavidin).

Results

Presentation of OVA Peptides Introduced by Osmotic Shock or Retrovirus Infection. To monitor MHC class I antigen processing pathway, we used a well-characterized K^b-restricted $OVA_{257–264}$ dominant antigen. Graded doses of synthetic peptides extending COOH-terminally ($OVA_{257–269}$), NH_2-terminally ($OVA_{248–264}$), or both sides of the epitope ($OVA_{248–269}$) were osmotically introduced into EL4 cells. Alternatively, these peptides were ectopically expressed by infection of a retrovirus encoding each of these peptides. Then, antigen presentation was measured by a standard ^{51}Cr-release CTL assay using CTLs specific for $OVA_{257–264}$. As shown in Fig. 1 a, cytolysis was dependent on the dose of peptides and on the virus titers. Cytolysis was observed in RMA cells, but not in TAP-2-mutated RMA-S cells (Fig. 1 b), indicating that the presentation of $OVA_{248–269}$ is TAP-dependent. In addition, a proteasome inhibitor LC completely abolished the killing of EL4 cells expressing $OVA_{257–269}$ and $OVA_{248–269}$, but not $OVA_{248–264}$ (Fig. 1 b), indicating that the proteasome is involved in the processing of COOH- but not NH_2-terminally extended peptides, as reported previously (30).

Enhanced Presentation of OVA Peptide by PA28α and hsp90. Next, we examined the roles of hsp90 and PA28 on OVA antigen presentation. Loading of hsp90, rPA28α,

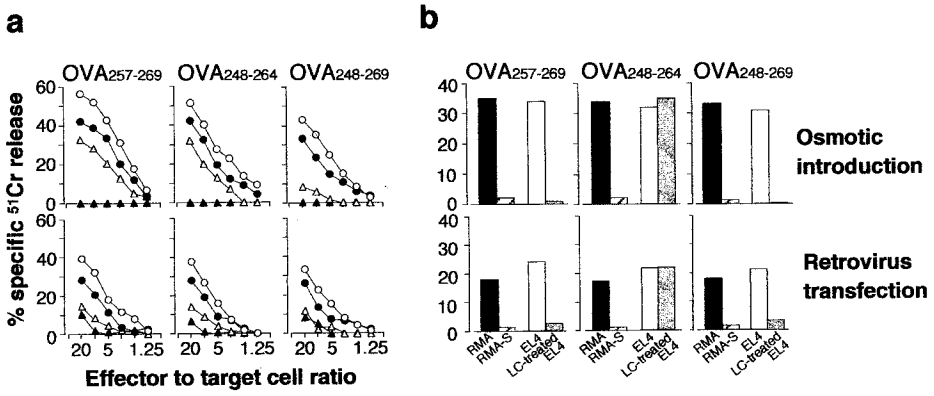

Figure 1. Presentation of OVA peptides introduced by osmotic shock or retrovirus transfection. (a) Dose-dependent effects of OVA peptides for CTL assay. (Top panel) EL4 cells were osmotically loaded with graded doses of synthetic peptides. 30 μg (○), 10 μg (●), 1 μg (Δ), 0.1 μg (▲). 30 μg of $OVA_{257–269}$, $OVA_{248–264}$, or $OVA_{248–269}$ corresponds to 19.1 nmol, 15.4 nmol, or 11.7 nmol, respectively. (Bottom panel) EL4 cells were transfected for 3 h by pMSCV retrovirus vector encompassing mini-genes encoding $OVA_{257–269}$ (3×10^7 CFU/ml), $OVA_{248–264}$ (3×10^7 CFU/ml), or $OVA_{248–269}$ (10^7 CFU/ml). The titration of the supernatants used for transfection was 1 (○), 1/10 (●), 1/100 (Δ), and 1/500 (▲). These OVA-introduced EL4 cells were labeled with $Na_2{}^{51}CrO_4$ and used as targets for lysis by $OVA_{257–264}$ specific CTLs. (b) TAP- and proteasome-dependency of OVA peptide presentation. $OVA_{257–269}$, $OVA_{248–264}$, and $OVA_{248–269}$ were osmotically introduced (4 nmol each peptide) or transfected (retrovirus solution: 3×10^6 CFU/ml) into 5×10^5 RMA, RMA-S, EL4, or LC (50 μM)-treated EL4 cells, as indicated. These cells were used as target cells for the CTL assay (E/T ratio = 10).

gp96, and hsc70 by osmotic shock resulted in ~2-3-fold increase of each protein in both the cytosol and membranous fractions of the EL4 cells compared with nonloaded cells (Fig. 2 a). $OVA_{248–269}$ was introduced with PA28α or hsp90 into EL4 cells by osmotic shock, and the presentation was assessed by CTL assay. Cytolysis was enhanced by hsp90 or PA28α but not by gp96, hsc70, or BSA (Fig. 2 b). We then examined the effects of GA or HA. Pretreatment of hsp90 with GA or HA in vitro abrogated the effect of hsp90, indicating the ATPase activity of hsp90 is required for hsp90-mediated antigen presentation. Although gp96, which is an endoplasmic reticulum (ER) resident member of Hsp90 family, is known to have a peptide chaperoning property similar to hsp90, it did not show any effect, suggesting that hsp90-assisted presentation is not simply due to its activity as a molecular chaperone that may protect the peptides from nonspecific degradation. It was previously reported that hsp90-peptide complex is

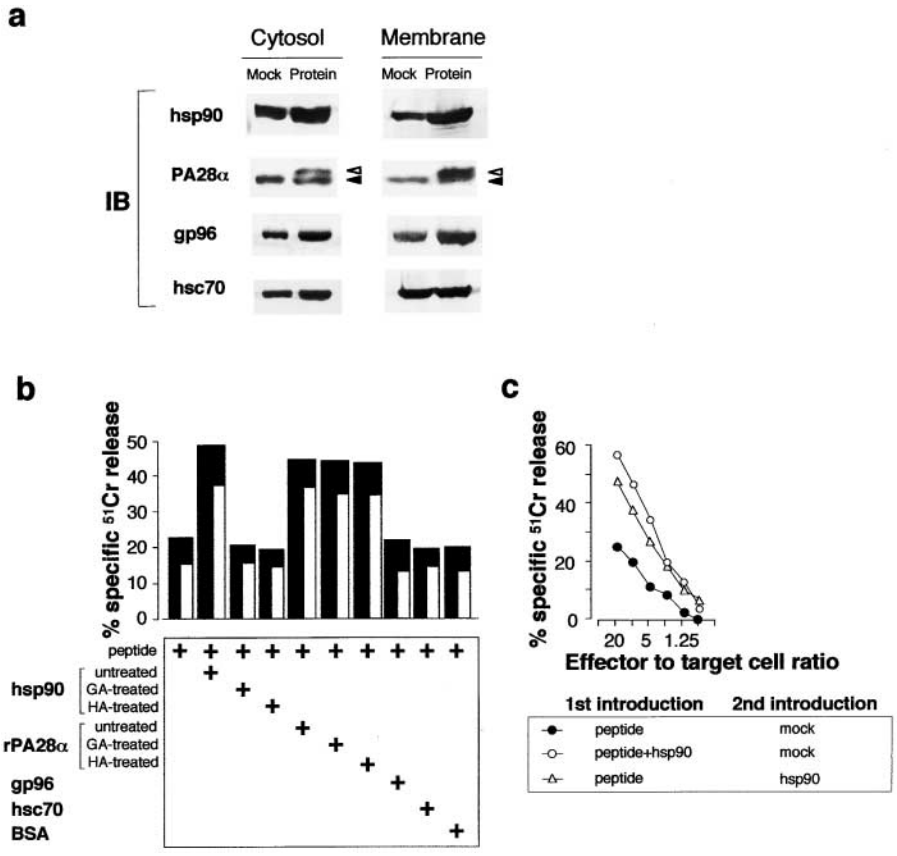

Figure 2. Effects of hsp90 and PA28α on $OVA_{248–269}$ peptide presentation. (a) Levels of introduced proteins. After osmotic introduction of hsp90, rPA28α, gp96, and hsc70 into EL4 cells, the cytosol and membrane fractions were used for Western blot analysis. Closed and open triangles indicate endogenous and rPA28α, respectively. (b) Augmentation by hsp90 and rPA28α on presentation of $OVA_{248–269}$ peptide. $OVA_{248–269}$ (3 nmol) was osmotically introduced into EL4 cells with or without hsp90, rPA28α, gp96, hsc70, and BSA. After hsp90 and rPA28α were treated for 1 h at 37°C with or without GA or HA in vitro, unbound ansamycin drugs were removed by extensive washing with PBS using an ultrafree-15 centrifugal filter device, before osmotic introduction and used for introduction, as indicated. These EL4 cells were used as target cells in CTL assay (E/T ratio 10 [■]; E/T ration 5 [□]). (c) The antigen processing after simultaneous or sequential introduction of $OVA_{248–269}$ and hsp90. $OVA_{248–269}$ was routinely introduced by admixing of the peptide and hsp90 (simultaneous introduction) into EL4 cells. For sequential introduction, after $OVA_{248–269}$ (3 nmol) was introduced and immediately after washing off the peptide, hsp90 was loaded into EL4 cells.

more active in antigen presentation than free peptides when loaded into cells, presumably due to its chaperone activity (31). To minimize the effect of hsp90 as a chaperone, we sequentially loaded peptide and hsp90 (first peptide, second hsp90), and cytolysis by CTLs was examined. As shown in Fig. 2 c, sequential loading obviously enhanced the presentation of the peptide compared with loading peptide alone and was comparable to that of admixing of Hsp90 and peptides. This result also suggests that hsp90 enhances antigen presentation in a novel fashion other than chaperoning peptides.

Accelerated Processing of COOH-terminally Extended Peptides by PA28α and hsp90. To further analyze the effects of PA28α and hsp90, we introduced the three OVA peptides with or without PA28α and hsp90 and measured antigen presentation by quantifying the cell-surface K^b-$OVA_{257–264}$ complex using mAb 25D.1–16 (28) as a function of time (at 0, 4, and 8 h). As shown in Fig. 3, a and b, when COOH-terminally extended peptides ($OVA_{257–269}$, $OVA_{248–269}$) were introduced without PA28α or hsp90, the cell surface expression of K^b-$OVA_{257–264}$ complex reached the maximum level 8 h after introduction, whereas cointroducing PA28α or hsp90 caused rapid presentation of the complex, resulting in maximum expression level after 4 h, although their intensities were nearly equal to each other. In contrast, NH_2-terminally extended peptide, $OVA_{248–264}$, was processed and presented regardless of the presence or absence of PA28α or hsp90. 12 h after peptide loading, the expression of K^b-$OVA_{257–264}$ complex in each case decreased (data not shown). Subsequently, we also performed CTL assay. Three peptides were introduced into EL4 cells either by osmotic shock or retrovirus infection together

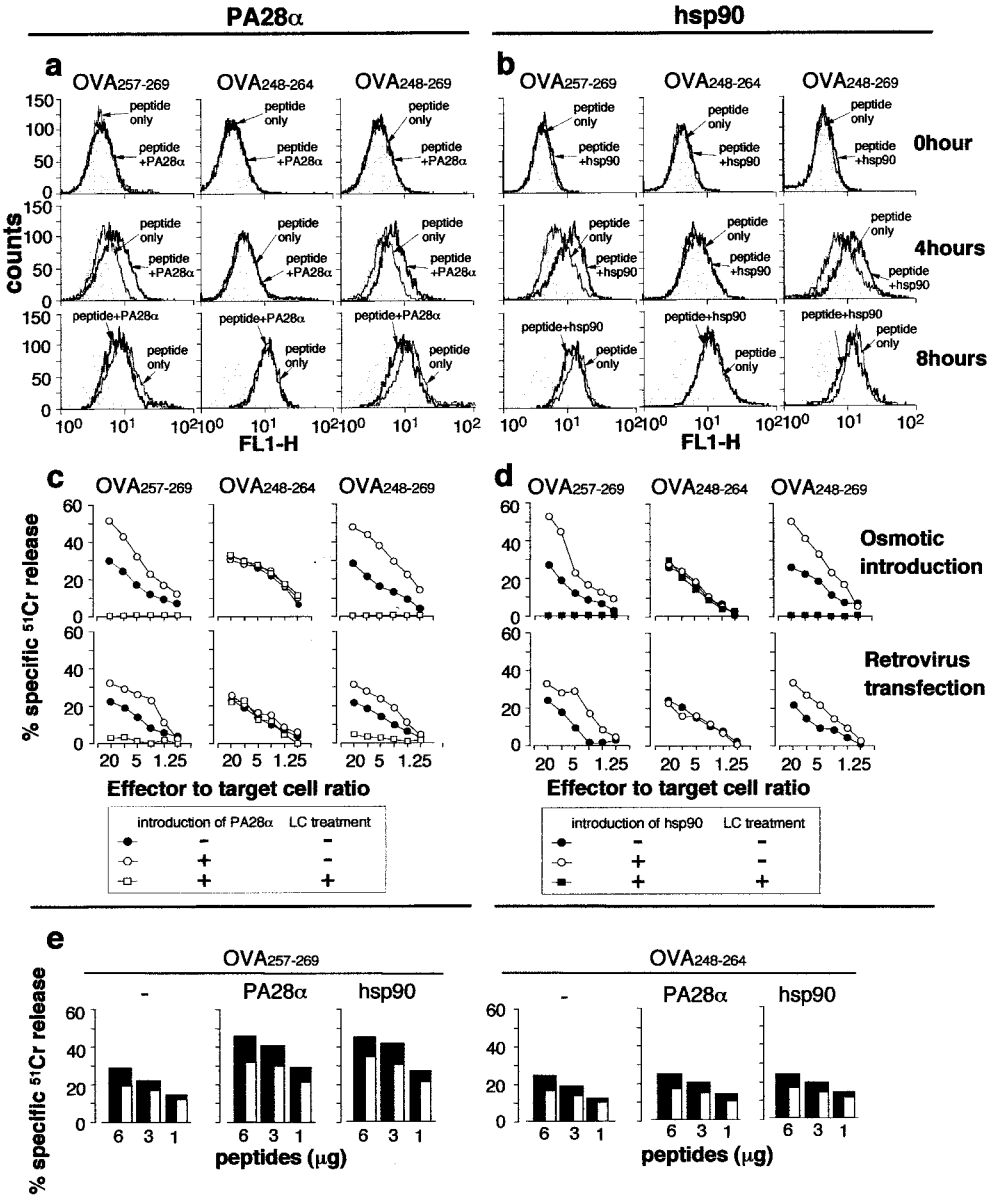

Figure 3. Hsp90 and PA28α augment the presentation of COOH- but not NH_2-terminally extended OVA peptides. (a and b) FACS® analysis. To obtain clear visualization of cell-surface K^b-$OVA_{257–264}$ complex, large amounts of $OVA_{257–269}$ (30 nmol), $OVA_{248–264}$ (30 nmol), and $OVA_{248–269}$ (25 nmol) peptides were introduced by osmotic shock, with or without rPA28α (a) or hsp90 (b). Staining with mAb 25.D1–16 followed by FITC-conjugated anti–mouse secondary Abs was performed 0, 4, and 8 h after introduction. Gray shadows indicate staining only with secondary Abs. (c and d) CTL assay. $OVA_{257–269}$, $OVA_{248–264}$, and $OVA_{248–269}$ (4 nmol each) were osmotically introduced or transfected by retrovirus solution with or without rPA28α (c) or hsp90 (d) into EL4 cells pretreated with or without LC (50 μM). For retrovirus transfection, EL4 cells were infected for 3 h by retrovirus solution (3×10^6 CFU/ml) immediately after osmotic introduction of rPA28α or hsp90. These cells were used as target cells in CTL assay. (e) Dose-dependent effects of $OVA_{257–269}$ and $OVA_{248–264}$ peptides for CTL assay. $OVA_{257–269}$ and $OVA_{248–264}$ were titrated as indicated and osmotically introduced into EL4 cells with or without rPA28α and hsp90, then the cytolysis by CTLs was determined. These EL4 cells were used as target cells in CTL assay (E/T ratio 10 [■]; E/T ratio 5 [□]).

with rPA28α or hsp90. rPA28α (Fig. 3 c) or hsp90 (Fig. 3 d) enhanced the cytolysis of cells expressing COOH- but not NH_2-terminally extended peptides. These enhancements by both proteins were completely abolished when EL4 cells were pretreated with LC, suggesting that hsp90 as well as rPA28α are functionally linked to the activity of the 20S proteasome. As shown in Fig. 3 e, PA28α and hsp90 appreciably augmented the processing of $OVA_{257–269}$, at any concentration of the peptides, while they had no effect on the processing of $OVA_{248–264}$ even at a limiting concentration. These data indicate that PA28 and hsp90 accelerate the processing of the COOH-terminally extended OVA peptides by the proteasome without changing its substrate specificities. It is of note that hsp90 did not affect the presentation of NH_2-terminally extended peptide, precluding again the effect of hsp90 as peptide chaperone and indicating that hsp90 acts through the function of the proteasome as PA28.

Geldanamycin Suppresses OVA Presentation in LPS Blasts Derived from PA28α$^{-/-}$/β$^{-/-}$ But Not PA28α$^{+/+}$/β$^{+/+}$ Mice. We next examined the epistasis of PA28- and hsp90-mediated pathways. We previously reported that the generation of $OVA_{257–264}$ epitope is not affected in PA28α$^{-/-}$/β$^{-/-}$ LPS blasts (15) and expression of total K^b of LPS blasts derived from PA28α$^{+/+}$/β$^{+/+}$ and PA28α$^{-/-}$/β$^{-/-}$ mice is almost comparable (data not shown), suggesting that there exists an alternative pathway for antigen processing, which compensates for the loss of PA28 in PA28α$^{-/-}$/β$^{-/-}$ LPS blasts. To test whether hsp90 acts in place of PA28 in these cells, LPS blasts from PA28α$^{+/+}$/β$^{+/+}$ and PA28α$^{-/-}$/β$^{-/-}$ mice were treated for 1.5 h with GA before osmotic loading of the three OVA peptides, and antigen presentation was monitored by CTL assay. Consistent with our previous report (15), the generation of $OVA_{257–264}$ epitope was not influenced by the absence of PA28. Furthermore, GA had no effect on PA28α$^{+/+}$/β$^{+/+}$ cells. Surprisingly, the processing of COOH-terminally extended peptides was profoundly inhibited by GA in PA28α$^{-/-}$/β$^{-/-}$ blasts (Fig. 4 a, top and middle panels). GA had no effect on the presentation of NH_2-terminally extended peptide ($OVA_{248–264}$) irrespective of the presence of PA28αβ. To examine whether the role of hsp90 is restricted in PA28α$^{-/-}$/β$^{-/-}$ LPS blasts or generally observed in other cells, we assessed the OVA epitope presentation in EL4 cells pretreated with GA or HA. As shown in Fig. 4 a (bottom panel), partial inhibition by GA or HA was observed in EL4 cells loaded with $OVA_{257–269}$ or $OVA_{248–269}$, but not in cells loaded with $OVA_{248–264}$.

To verify that the loaded peptide $OVA_{248–264}$ were processed and presented internally in cells, we treated LPS blasts and EL4 cells with BFA during antigen processing and performed CTL assay. BFA treatment completely inhibited the presentation of the peptide, and pulsing of the epitope peptide to BFA treated cells restored the cytolysis (Fig. 4 b). The processing of COOH-terminally extended peptides $OVA_{257–269}$ or $OVA_{248–269}$ was also inhibited by BFA (data not shown) like LC (Fig. 3, c and d), indicating that all peptides used were processed and presented internally in cells.

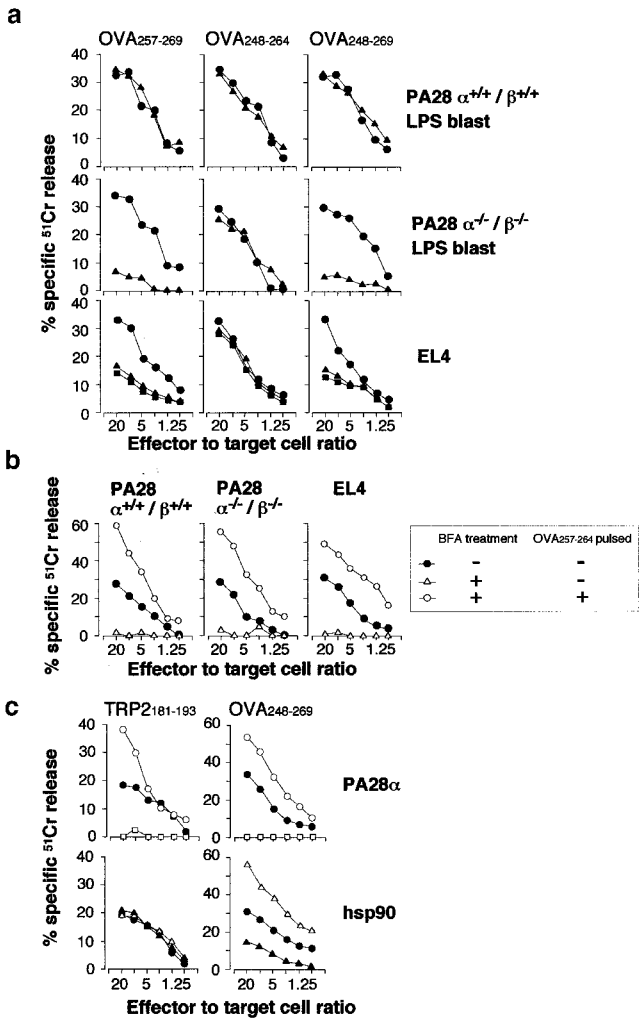

Figure 4. Effects of geldanamycin on antigen presentation in PA28α$^{-/-}$/β$^{-/-}$ and PA28α$^{+/+}$/β$^{+/+}$ blasts and EL4 cells. (a) $OVA_{257–269}$, $OVA_{248–264}$, and $OVA_{248–269}$ (4 nmol each) were osmotically introduced into LPS blasts of PA28α$^{+/+}$/β$^{+/+}$ and PA28α$^{-/-}$/β$^{-/-}$ mice or EL4 cells pretreated with GA (▲) or HA (■) or untreated (●) for 1.5 h. These cells were used as target cells in CTL assay. (b) BFA dependency on antigen presentation. $OVA_{248–264}$ was osmotically introduced into EL4 cells pretreated with (Δ) or without (●) 5 μg/ml BFA. BFA was treated 1 h before the introduction of peptide and continued for 3 h with (○) or without (Δ, ●) pulsation of $OVA_{257–264}$ in EL4 cells. The ^{51}Cr-release assay was performed as in panel a. (c) $TRP2_{181–193}$ and $OVA_{248–269}$ (4 nmol each) were osmotically introduced, with PA28α (○), hsp90 (Δ), or alone (●) into EL4 cells pretreated with GA (▲) or LC (□) for 1.5 h. These cells were used as target cells in CTL assay.

These results indicate that the hsp90-dependent processing pathway is common, but the contribution of hsp90 in antigen processing seems to depend on the cell type. As reported previously (15), PA28α$^{-/-}$/β$^{-/-}$ LPS blasts almost completely lost the ability to process a melanoma antigen TRP-2 peptide ($TRP2_{181–188}$), indicating that PA28 is definitely required for this antigen presentation. Considering the partial suppression by GA or HA for $OVA_{257–264}$ pre-

sentation in EL4 cells, it is interesting to test how PA28 or hsp90 affects the $TRP2_{181–188}$ presentation in these cells. We introduced $TRP2_{181–193}$ (COOH-terminally extended) or $OVA_{248–269}$, together with rPA28α or hsp90, into EL4 cells pretreated with or without GA. As shown in Fig. 4 c, neither hsp90 nor GA-treatment influenced the presentation of $TRP2_{181–188}$, whereas rPA28α considerably increased the presentation of this epitope, suggesting that presentation of $TRP2_{181–188}$ is absolutely dependent on PA28 and that hsp90 does not have any role for this epitope. On the other hand, experiments using $OVA_{248–269}$ again showed that both PA28α and hsp90 contributed to the presentation of the epitope in EL4 cells (Fig. 4 c), indicating that these two pathways operate in these cells. Taken together, the PA28- and the hsp90-dependent pathways for antigen processing can work both redundantly and specifically, which depends on the type of antigen.

IFN-γ Increases Dependency on PA28 Rather Than hsp90. It is clear that both the PA28- and hsp90-dependent pathways for OVA epitope presentation operate redundantly in wild-type LPS blasts and EL4 cells, but the PA28-dependent pathway seems to be dominant in LPS blasts compared with EL4 cells, based on GA sensitivity. The difference may be due to the balance of PA28 and hsp90 expression. Therefore, we next examined the effect of IFN-γ on the two pathways of antigen processing in E.G7 cells, which express the full-length OVA protein. We transfected retrovirus vectors encoding cDNAs of either PA28α or hsp90 into E.G7 cells, and measured the cell-surface quantity of K^b-$OVA_{257–264}$, with or without GA and/or IFN-γ treatment. The total cell extracts from these transfected cells resulted in 2–3-fold increase in hsp90 or PA28α, as determined by densitometric analysis (Fig. 5 a, top panel). Whereas both PA28α and hsp90 enhanced the expression of K^b-$OVA_{257–264}$ complex, the stimulatory effect of hsp90, was completely prevented by GA treatment, unlike PA28α (Fig. 5 b). Interestingly, preincubation with IFN-γ for 24 h markedly induced both PA28α and PA28β (Fig. 5 a, bottom panel), and at the same time almost completely abrogated the inhibitory effect of GA (Fig. 5 b).

This observation was further confirmed by an acid-wash recovery assay. E.G7 cells preincubated with or without IFN-γ were briefly exposed to acid medium (pH 3.0) in order to destroy surface MHC-peptide complexes of cells, and then monitored the recovery of K^b-$OVA_{257–264}$ complex expression. As shown in Fig. 5 c, GA significantly sup-

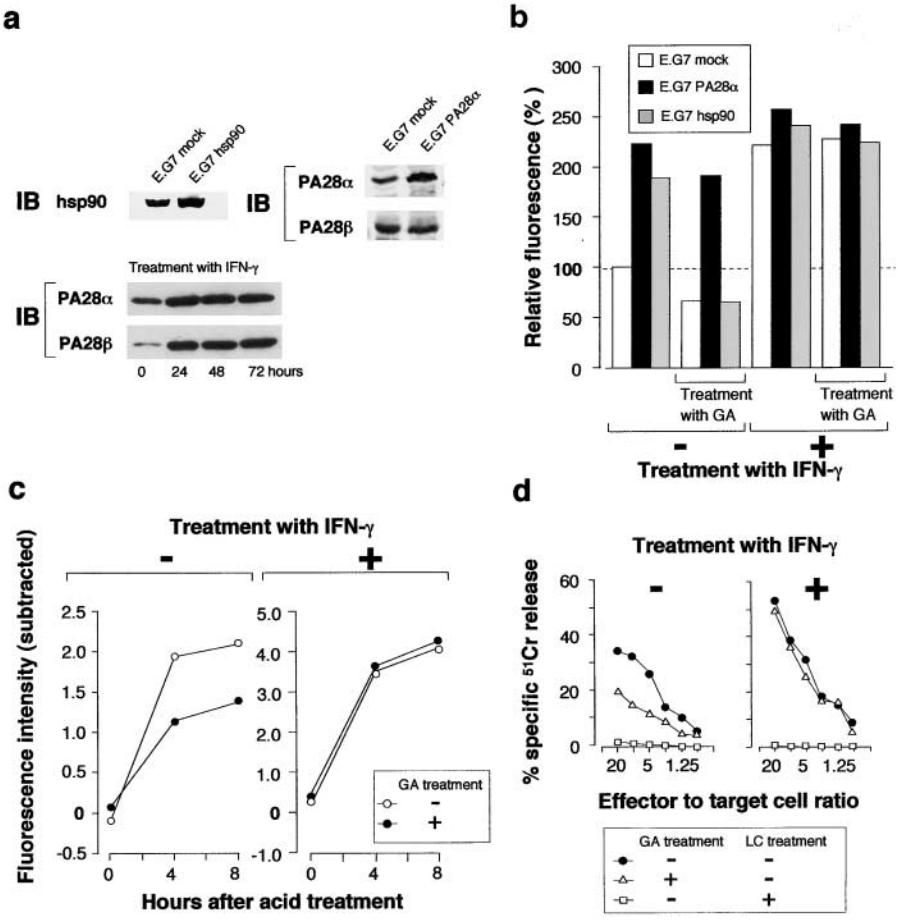

Figure 5. Effects of geldanamycin and IFN-γ on K^b-$OVA_{257–264}$ complex expression and CTL assay. (a) Levels of expressed proteins. The hsp90, PA28α, and PA28β in total cell extracts of E.G7 mock, E.G7 hsp90, E.G7 PA28α that had been prepared by dissolving with the sample buffer for SDS-PAGE were examined by Western blot analysis. The expression of PA28α and β were examined after culture with IFN-γ (50 U/ml) for the indicated periods. All the quantity of each protein was assessed by densitometric analysis of ECL-exposed films. (b) FACS® analysis in OVA-expressing E.G7 cells. E.G7 cells were transfected with retrovirus vector containing cDNA of PA28α or hsp90 or mock and established, as described in Materials and Methods. These cells were incubated in the presence or absence of IFN-γ (50 U/ml) for 36 h. During the last 12 h of incubation, the cells were treated with or without GA (5 μM), and stained with mAb 25D.1–16 for the analysis of the expression of K^b-$OVA_{257–264}$ complex by FACS® and the results are shown as relative fluorescence. (c) Acid wash recovery assay. E.G7 cells that had been preincubated in the presence or absence of IFN-γ (50 U/ml) for 36 h were acid (pH 3.0) treated. The E.G7 cells were cultured with GA (●), without (○) GA 1 h before acid washing and during the following incubation in the presence or absence of IFN-γ, then the expression of K^b–$OVA_{257–264}$ complex was examined with mAb 25D.1–16 at indicated periods after acid treatment. (d) CTL assay in EL4 cells. $OVA_{248–269}$ (4 nmol) was osmotically introduced into EL4 cells pretreated with or without GA or LC (50 μM). These cells were used as target cells in a ^{51}Cr-release assay. The same experiment was also performed with EL4 cells that had been cultured with 50 U/ml IFN-γ for 24 h.

pressed the recovery of K^b-$OVA_{257–264}$ complex, but this suppression was cancelled by treatment with IFN-γ. These results were also confirmed by CTL assays, in which $OVA_{248–269}$ was introduced into EL4 cells pretreated with or without GA. As shown in Fig. 5 d, GA considerably inhibited OVA presentation in EL4 cells that were not treated with IFN-γ, whereas no significant suppression of cytolysis by GA was observed when EL4 cells were cultured in the presence of IFN-γ for 24 h before subjected to the CTL assay.

We also tested the expression of total K^b molecules on cell surface of E.G7 cells transfected with mock, PA28α or hsp90 cDNA. To exclude the possible nonspecific influence of GA on the stability of cell-surface molecules, we also examined the surface expression of LFA-1. As shown in Fig. 6 a, K^b expression was significantly suppressed by GA, especially in E.G7 hsp90, whereas that of LFA-1 was not affected. The GA-dependent reduction of K^b was completely restored to the level of E.G7 mock cells by incubation with the K^b ligand $OVA_{257–264}$ (Fig. 6 b), indicating that the reduction of K^b was due to a disturbed supply of K^b ligands. Incubation of E.G7 cells with IFN-γ greatly enhanced the expression of surface K^b molecules, which could not be inhibited by GA (Fig. 6 b). These results were further confirmed by an acid-wash recovery assay as mentioned above. As shown in Fig. 6 c, GA significantly inhibited the recovery of K^b, which was restored by incubation with the epitope peptides, but IFN-γ abrogated the inhibition.

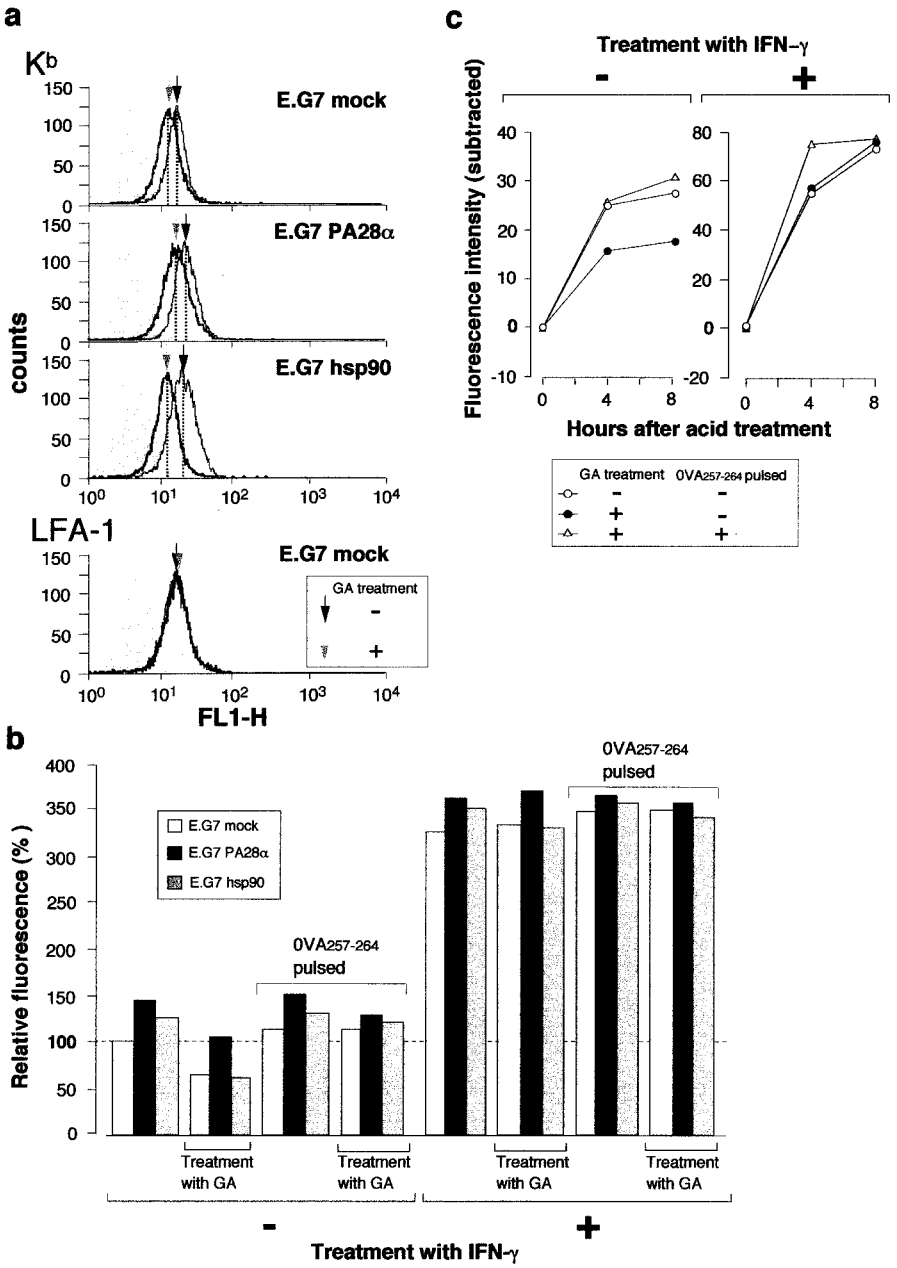

Figure 6. Effects of geldanamycin and IFN-γ on total K^b expression in E.G7 cells. (a and b) Expression of K^b and LFA-1 molecules. E.G7 mock, E.G7 PA28α, and E.G7 hsp90 cells were cultured in the presence or absence of GA (5 μM) with or without $OVA_{257–264}$ (10 μg/ml), for 12 h. The expression of K^b and LFA-1 molecules on these cells was examined with biotin-conjugated mAb CTKb and M17/4.2, respectively, followed by staining with avidin-FITC. Results are shown as a histogram (a) and as relative mean fluorescence (b). The experiments were also performed with the transfectants, which were precultured in the presence of IFN-γ for 24 h. In a, the gray shadows indicate staining only with avidin-FITC. (c) Acid-wash recovery assay. E.G7 cells were treated with acid in the presence or absence of IFN-γ as in Fig. 5 c. The E.G7 cells were cultured with GA (●), GA and $OVA_{257–264}$ (Δ), without (○) GA 1 h before acid washing and during the following incubation in the presence or absence of IFN-γ, then the expression of total K^b was examined at indicated periods after acid treatment.

These results suggest that IFN-γ treatment reduces the contribution of the hsp90-dependent processing pathway.

Finally, we examined whether IFN-γ can induce the cell surface expression of K^b molecules in cells derived from PA28$\alpha^{-/-}/\beta^{-/-}$ mice. To this end, peritoneal macrophages (Mϕ) were prepared from PA28$\alpha^{-/-}/\beta^{-/-}$ mice and tested for K^b expression on their cell surfaces. IFN-γ markedly enhanced cell surface K^b expression in wild-type Mϕ, however, no induction of K^b was observed in PA28$\alpha^{-/-}/\beta^{-/-}$ Mϕ (Fig. 7, a and b) and pulsing of $OVA_{257–264}$ peptides to IFN-γ–treated PA28$\alpha^{-/-}/\beta^{-/-}$ Mϕ markedly increased the expression of K^b to a level comparable with that of wild-type cells (Fig. 7 b). These results indicate that PA28-deficient cells induce K^b molecules as well as wild-type cells upon IFN-γ stimulation, but that K^b ligands were not supplied in sufficient amount in PA28-deficient cells. In other words, PA28-dependent pathway is the main route responsible for antigen processing when cells were stimulated with IFN-γ. Another important feature is the profound inhibition of K^b expression by GA in IFN-γ-treated PA28$\alpha^{-/-}/\beta^{-/-}$ Mϕ, which was in contrast to that in wild-type Mϕ (Fig. 7 b). Similar results were obtained

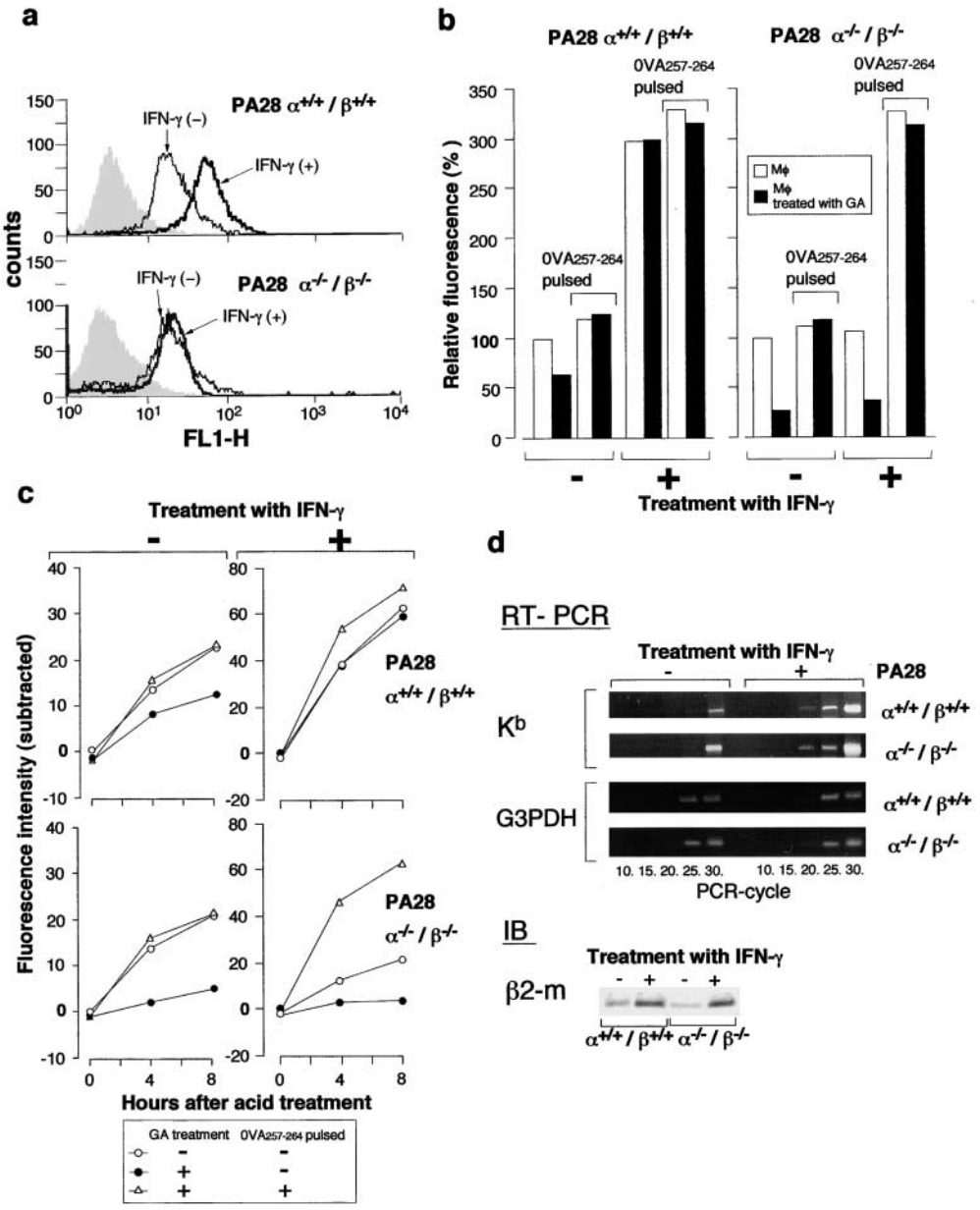

Figure 7. Lack of IFN-γ–dependent induction of cell surface K^b molecules in macrophages derived from PA28$\alpha^{-/-}/\beta^{-/-}$ mice. (a) Effects of IFN-γ on K^b expression in peritoneal macrophages of PA28$\alpha^{+/+}/\beta^{+/+}$ and PA28$\alpha^{-/-}/\beta^{-/-}$ mice. Peritoneal macrophages (Mϕ) of PA28$\alpha^{+/+}/\beta^{+/+}$ or PA28$\alpha^{-/-}/\beta^{-/-}$ mice were incubated in the presence or absence of IFN-γ for 48 h and the resulting cell surface expression of K^b was examined with FACS® analysis as indicated by arrows. (b) Effects of $OVA_{257–264}$ pulse of K^b expression on Mϕ from PA28$\alpha^{+/+}/\beta^{+/+}$ and PA28$\alpha^{-/-}/\beta^{-/-}$ mice. These macrophages were treated with or without GA for the last 12 h of incubation in the presence or absence of $OVA_{257–264}$ peptide simultaneously. The results obtained are represented as histograms showing the relative fluorescence. (c) Acid wash recovery assay. Peritoneal macrophages of PA28$\alpha^{+/+}/\beta^{+/+}$ or PA28$\alpha^{-/-}/\beta^{-/-}$ mice were treated with acid in the presence or absence of IFN-γ as in Fig. 5 c. These cells were cultured with GA (●), GA and $OVA_{257–264}$ (Δ), without (○) GA 1 h before acid wash and during the following incubation in the presence or absence of IFN-γ, then the expression of total K^b was examined at indicated periods after acid treatment. (d) Effect of IFN-γ on the expression of K^b and β_2-m in PA28–deficient MEFs. The expression of heavy chain (K^b) and β_2 microglobulin (β_2-m) of embryonic fibroblasts (MEFs) of PA28$\alpha^{+/+}/\beta^{+/+}$ and PA28$\alpha^{-/-}/\beta^{-/-}$ mice was induced by IFN-γ. RNAs for RT-PCR were extracted from MEFs of PA28$\alpha^{+/+}/\beta^{+/+}$ and PA28$\alpha^{-/-}/\beta^{-/-}$ mice that had been cultured in the presence or absence of IFN-γ (50 U/ml) for 48 h and 40 and 4 ng RNA was used for RT-PCR of K^b and G3PDH, respectively. The RT-PCR products of K^b and G3PDH after 10 to 30 cycles were run onto 2% agarose gel electrophoresis and stained with ethylene bromide. Total cell lysates for immunoblotting (IB) were prepared from 8×10^4 MEFs of PA28$\alpha^{+/+}/\beta^{+/+}$ and PA28$\alpha^{-/-}/\beta^{-/-}$ mice that had been treated with IFN-γ as mentioned above. The lysates were run on a 15% SDS-PAGE, transferred to a nitrocellulose membrane followed by blotting with specific antibody.

using both bone marrow–derived dendritic cells and MEFs (data not shown). These intriguing observations were confirmed by the acid-wash recovery assay. Indeed, in the absence of IFN-γ, GA completely inhibited the recovery of K^b expression on Mϕ of PA28$\alpha^{-/-}/\beta^{-/-}$ and partially of PA28$\alpha^{+/+}/\beta^{+/+}$, which was restored by incubation with pulsing of $OVA_{257–264}$. Treatment with IFN-γ significantly enhanced the level of K^b expression of wild-type Mϕ and the enhanced K^b expression was not inhibited by GA. On the other hand, IFN-γ treatment of PA28$\alpha^{-/-}/\beta^{-/-}$ Mϕ did not enhance K^b expression, although $OVA_{257–264}$ pulsing enhanced the K^b expression to a level similar to that of the wild-type cells treated with IFN-γ (Fig. 7 c). The expression of heavy chain of K^b and β_2 microglobulin was normally induced by IFN-γ in MEFs derived from PA28$\alpha^{-/-}/\beta^{-/-}$ mice, as assessed by RT-PCR and Western blotting, respectively (Fig. 7 d), which is consistent with the enhancement of K^b expression when $OVA_{257–264}$ was pulsed. Furthermore, GA treatment completely inhibited K^b expression on PA28$\alpha^{-/-}/\beta^{-/-}$ Mϕ even when they were treated by IFN-γ. In addition, there was no difference in TAP2 induction by IFN-γ between wild-type and PA28-deficient cells (data not shown), showing IFN-γ signaling and MHC class I assembly components were apparently normal in PA28-deficient mice. Taken together, our results indicate that in IFN-γ treated cells PA28-dependent pathway is dominant for epitope supply to MHC class I molecules, whereas hsp90-dependent pathway becomes negligible, even for epitopes processed by both pathways under normal circumstances such as OVA.

Discussion

In this study, we provide evidence to show the existence of two distinct pathways responsible for generation of MHC class I ligands, one is hsp90 dependent and the other PA28 dependent. These two pathways were clearly characterized by using hsp90-specific inhibitors GA and HA and cells derived from PA28$\alpha^{-/-}/\beta^{-/-}$ mice. Our results showed that antigen presentation in LPS blasts of PA28$\alpha^{-/-}/\beta^{-/-}$ mice was profoundly inhibited by GA, whereas GA never and only partially inhibited the generation of $OVA_{257–264}$ epitope in PA28-positive LPS blasts and EL4 cells, respectively, indicating that these two pathways cooperate in these cells (Fig. 4 a). In contrast, in the absence of GA treatment, the generation of OVA epitope was not impaired in PA28$\alpha^{-/-}/\beta^{-/-}$ blasts and rather comparable to that of PA28$\alpha^{+/+}/\beta^{+/+}$ blasts (Fig. 4 a), consistent with our previous findings (15). In addition, the presentation of $OVA_{257–264}$ epitope from native OVA was clearly enhanced by PA28α and hsp90 (Fig. 5 b). The enhancement by hsp90 but not by PA28α was almost completely inhibited by GA, indicating that the ATPase activity of hsp90 is required for antigen presentation although GA inhibits not only hsp90 but also gp96 in the ER. Taken together, our results indicate that PA28 and hsp90 redundantly contribute to the $OVA_{257–264}$ epitope-processing pathway. It is clear that hsp90 plays an essential role in the presentation of $OVA_{257–264}$ epitope in the absence of PA28, which was clearly demonstrated using GA-treated PA28$\alpha^{-/-}/\beta^{-/-}$ LPS blasts, whereas PA28 is dominant in PA28$\alpha^{+/+}/\beta^{+/+}$ LPS blasts.

On the other hand, presentation of $TRP2_{181–188}$ epitope was solely dependent on PA28, even in the presence of hsp90 in PA28$\alpha^{-/-}/\beta^{-/-}$ LPS blasts. Consistent with this observation, rPA28α had a stimulatory effect on the $TRP2_{181–188}$ processing in EL4 cells, whereas introduction of hsp90 and GA treatment had no effect (Fig. 4 c, left panel). Taken together, it is concluded that the two pathways mediated by hsp90 and PA28 redundantly contribute to OVA processing, but the $TRP2_{181–188}$ epitope processing is specifically mediated by the PA28-dependent pathway. Thus, it appears that utilization of these two pathways is dependent on antigen species.

In wild-type LPS blasts and EL4 cells treated with IFN-γ, the PA28-dependent pathway is dominant, as GA had no obvious inhibitory effects on $OVA_{257–264}$ epitope generation (Figs. 4 a and 5, b–d). It is possible that the PA28-dependent pathway suppresses the hsp90-dependent pathway for processing of the same antigens. To understand this phenomenon, it is essential to determine the molecular mechanism of hsp90 involved in the MHC class I ligand production. How can hsp90 activate antigen processing? We first investigated whether hsp90 enhanced peptide hydrolyzing activity of the proteasome like PA28 in vitro, but the results showed it did not (data not shown), consistent to the previous reports (19, 20). In this regard, Goasduff and Cederbaum (32) have recently reported that hsp90 inhibited the cleavage of the fluorogenic peptide by purified proteasome in vitro, whereas the use of hsp90 and cytosolic fraction enhanced the hydrolysis, suggesting that hsp90 together with other unidentified cytosolic factors could activate the hydrolysis by the proteasome. Furthermore, several studies have shown the binding of hsp90 to the 20S proteasome (19, 20, and unpublished data). In considering the redundant roles between PA28 and hsp90 pathways, hsp90 (with or without other proteins) might be directly involved in proteasome-dependent processing of antigens by forming a complex with 20S proteasome, as PA28 does. This model may explain in part the dominance of the PA28 over hsp90, although the role of the hsp90-proteasome complex remains to be determined.

The results shown in Fig. 3, c and d, also suggested the linkage of hsp90 and the proteasome. COOH- and NH_2-terminally extended $OVA_{248–269}$ was presented more efficiently than only NH_2-terminally extended $OVA_{248–264}$ by PA28 and hsp90, while lactacystin blocked only the presentation of COOH-terminally extended peptides. This suggests a mechanism that facilitates delivery of peptides processed by the proteasome to the MHC class I assembly system on the ER. In this regard, it is interesting that proteasomes, PA28, and hsp90 are associated with the ER membranes, probably the cytosolic face (33, 34), imaging a speculative model that the proteasome processing machinery involving PA28 and hsp90 may be directly linked to

the TAP antigen transport system, as proposed previously by Rechsteiner et al. (6). One may attribute the effect of hsp90 to its function as a peptide carrier. Although we showed in this study that enhanced processing of OVA peptides by hsp90 was not attributed to its role as a peptide chaperone because hsp90 did not affect the presentation of NH_2-terminally extended peptide and that the effect of hsp90 was exactly linked to the proteasome, it is still possible that hsp90 plays a role as post-proteasomal peptide carrier. That is, hsp90 might bind peptides generated by the proteasome and safely carry them to TAP transporter, preventing further degradation by cytosolic peptidases as suggested by Binder et al. (31). Indeed, when hsp90 and PA28 were osmotically introduced, their levels were increased 2–3-fold in the cytosol as well as the membranous fractions (Fig. 2 a). Therefore, considerable amounts of transfected proteins are thought to be associated with the membranes, probably the ER, as considerable amounts of hsp90 and PA28 were recovered in the membrane fractions in cells, even without osmotic loading of these proteins (Fig. 2 a).

Another important aspect of the two distinct pathways is their physiological roles. In this study, we provided evidence that the PA28 pathway is up-regulated by IFN-γ. In this context, we propose the existence of a constitutive pathway and adaptive pathway regulated by IFN-γ in MHC class I antigen processing. The process requiring hsp90 can be regarded as a constitutive pathway. On the other hand, the PA28-mediated pathway can be regarded as an adaptive pathway, because PA28 is markedly induced by a major cytokine IFN-γ. In fact, we showed that GA had no significant effect on $OVA_{257–264}$ epitope generation in PA28$\alpha^{+/+}/\beta^{+/+}$ LPS blasts (Fig. 4 a). This is probably because the PA28$\alpha^{+/+}/\beta^{+/+}$ LPS blasts express a large amount of PA28, and hence the hybrid proteasome. Consistent with this model, GA had no effect on $OVA_{257–264}$ epitope generation in IFN-γ–treated EL4 cells, nevertheless it considerably inhibited the presentation in E.G7 cells without treatment with IFN-γ (Fig. 5, b and c). In addition, GA treatment of E.G7 cells down-regulated the expression of total K^b molecules (Fig. 6) as well as K^b-$OVA_{257–264}$ complex on the cell surface (Fig. 5, b and c). Conversely, transfection of hsp90 cDNA by retrovirus enhanced cell surface K^b molecules (Fig. 6 b) and other tumor cell lines (data not shown). Regarding the expression of K^b-$OVA_{257–264}$ complex and total K^b, the inhibitory effect by GA was abolished by incubation of cells with IFN-γ (Fig. 5, b and c, and Fig. 6, b and c). Thus, IFN-γ shifts the functional balance from hsp90 toward PA28. The defect of IFN-γ–induced up-regulation of K^b molecules on cell surface of macrophages (Fig. 7), dendritic cells, MEFs, and LPS blasts (data not shown) derived from PA28$\alpha^{-/-}/\beta^{-/-}$ mice also supports this notion. The reason for this shift could attribute to the fact that IFN-γ can induce PA28, resulting in an increase in the hybrid-proteasome (9). As hsp90 was not induced by IFN-γ (data not shown), the substantial role of hsp90 in antigen presentation would be replaced by abundant PA28. Indeed, down-regulation of total K^b molecules by GA was markedly enhanced even in IFN-γ–treated macrophages of PA28$\alpha^{-/-}/\beta^{-/-}$ mice (Fig. 7 b), which was in contrast to that of wild-type mice.

In summary, we have reported a novel function for hsp90, and demonstrated the crucial role of PA28 on IFN-γ–induced up-regulation of MHC class I molecules. Our results provide fundamental insight into the function of PA28 and hsp90 in MHC class I antigen processing/presentation.

We thank Ms. Hiroiwa for the excellent technical support, especially for preparation of recombinant proteins.

This work was supported by a Grant-in-Aid for Scientific Research on Priority Areas from the Ministry of Education, Science, Sports and Culture, Japan.

Submitted: 16 November 2001
Revised: 10 May 2002
Accepted: 3 June 2002

References

1. Rock, K.L., and A.L. Goldberg. 1999. Degradation of cell proteins and the generation of MHC class I-presented peptides. *Annu. Rev. Immunol.* 17:739–779.
2. Tanaka, K., and M. Kasahara. 1998. The MHC class I ligand-generating system: roles of immunoproteasomes and the interferon-γ-inducible proteasome activator PA28. *Immunol. Rev.* 163:161–176.
3. Kloetzel, P.M. 2001. Antigen processing by the proteasome. *Nat. Rev. Mol. Cell Biol.* 2:179–187.
4. Bochtler, M., L. Ditzel, M. Groll, C. Hartmann, and R. Huber. 1999. The proteasome. *Annu. Rev. Biophys. Biomol. Struct.* 28:295–317.
5. Voges, D., P. Zwickl, and W. Baumeister. 1999. The 26S proteasome: a molecular machine designed for controlled proteolysis. *Annu. Rev. Biochem.* 68:1015–1068.
6. Rechsteiner, M., C. Realini, and V. Ustrell. 2000. The proteasome activator 11 S REG (PA28) and class I antigen presentation. *Biochem. J.* 345:1–15.
7. Song, X., J.D. Mott, J. von Kampen, B. Pramanik, K. Tanaka, C.A. Slaughter, and G.N. DeMartino. 1996. A model for the quaternary structure of the proteasome activator PA28. *J. Biol. Chem.* 271:26410–26417.
8. Zhang, Z., A. Krutchinsky, S. Endicott, C. Realini, M. Rechsteiner, and K.G. Standing. 1999. Proteasome activator 11S REG or PA28: recombinant REG α/REG β hetero-oligomers are heptamers. *Biochemistry.* 38:5651–5658.
9. Tanahashi, N., Y. Murakami, Y. Minami, N. Shimbara, K.B. Hendil, and K. Tanaka. 2000. Hybrid proteasomes. Induction by interferon-γ and contribution to ATP-dependent proteolysis. *J. Biol. Chem.* 275:14336–14345.
10. Dick, T.P., T. Ruppert, M. Groettrup, P.M. Kloetzel, L. Kuehn, U.H. Koszinowski, S. Stevanovic, H. Schild, and H.G. Rammensee. 1996. Coordinated dual cleavages induced by the proteasome regulator PA28 lead to dominant MHC ligands. *Cell.* 86:253–262.
11. Shimbara, N., H. Nakajima, N. Tanahashi, K. Ogawa, S. Niwa, A. Uenaka, E. Nakayama, and K. Tanaka. 1997. Double-cleavage production of the CTL epitope by proteasomes and PA28: role of the flanking region. *Genes Cells.* 2:785–800.
12. Groettrup, M., A. Soza, M. Eggers, L. Kuehn, T.P. Dick, H. Schild, H.G. Rammensee, U.H. Koszinowski, and P.M.

Kloetzel. 1996. A role for the proteasome regulator PA28α in antigen presentation. *Nature*. 381:166–168.
13. Preckel, T., W.P. Fung-Leung, Z. Cai, A. Vitiello, L. Salter-Cid, O. Winqvist, T.G. Wolfe, M. Von Herrath, A. Angulo, P. Ghazal, et al. 1999. Impaired immunoproteasome assembly and immune responses in PA28$^{-/-}$ mice. *Science*. 286: 2162–2165.
14. Fruh, K., and Y. Yang. 1999. Antigen presentation by MHC class I and its regulation by interferon γ. *Curr. Opin. Immunol.* 11:76–81.
15. Murata, S., H. Udono, N. Tanahashi, N. Hamada, K. Watanabe, K. Adachi, T. Yamano, K. Yui, N. Kobayashi, M. Kasahara, et al. 2001. Immunoproteasome assembly and antigen presentation in mice lacking both PA28α and PA28β. *EMBO J.* 20:5898–5907.
16. Buchner, J. 1999. Hsp90 & Co. - a holding for folding. *Trends Biochem. Sci.* 24:136–141.
17. Young, J.C., I. Moarefi, and F.U. Hartl. 2001. Hsp90: a specialized but essential protein-folding tool. *J. Cell Biol.* 154: 267–273.
18. Richter, K., P. Muschler, O. Hainzl, and J. Buchner. 2001. Coordinated ATP hydrolysis by the Hsp90 dimer. *J. Biol. Chem.* 276:33689–33696.
19. Tsubuki, S., Y. Saito, and S. Kawashima. 1994. Purification and characterization of an endogenous inhibitor specific to the Z-Leu-Leu-Leu-MCA degrading activity in proteasome and its identification as heat-shock protein 90. *FEBS Lett.* 344:229–233.
20. Wagner, B.J., and J.W. Margolis. 1995. Age-dependent association of isolated bovine lens multicatalytic proteinase complex (proteasome) with heat-shock protein 90, an endogenous inhibitor. *Arch. Biochem. Biophys.* 323:455–462.
21. Connell, P., C.A. Ballinger, J. Jiang, Y. Wu, L.J. Thompson, J. Hohfeld, and C. Patterson. 2001. The co-chaperone CHIP regulates protein triage decisions mediated by heat-shock proteins. *Nat. Cell Biol.* 3:93–96.
22. Young, J.C., C. Schneider, and F.U. Hartl. 1997. In vitro evidence that hsp90 contains two independent chaperone sites. *FEBS Lett.* 418:139–143.
23. Ishii, T., H. Udono, T. Yamano, H. Ohta, A. Uenaka, T. Ono, A. Hizuta, N. Tanaka, P.K. Srivastava, and E. Nakayama. 1999. Isolation of MHC class I-restricted tumor antigen peptide and its precursors associated with heat shock proteins hsp70, hsp90, and gp96. *J. Immunol.* 162:1303–1309.
24. Prodromou, C., S.M. Roe, R. O'Brien, J.E. Ladbury, P.W. Piper, and L.H. Pearl. 1997. Identification and structural characterization of the ATP/ADP-binding site in the Hsp90 molecular chaperone. *Cell.* 90:65–75.
25. Whitesell, L., E.G. Mimnaugh, B. De Costa, C.E. Myers, and L.M. Neckers. 1994. Inhibition of heat shock protein HSP90-pp60v-src heteroprotein complex formation by benzoquinone ansamycins: essential role for stress proteins in oncogenic transformation. *Proc. Natl. Acad. Sci. USA.* 91:8324–8328.
26. Udono, H., T. Yamano, Y. Kawabata, M. Ueda, and K. Yui. 2001. Generation of cytotoxic T lymphocytes by MHC class I ligands fused to heat shock cognate protein 70. *Int. Immunol.* 13:1233–1242.
27. Moore, M.W., F.R. Carbone, and M.J. Bevan. 1988. Introduction of soluble protein into the class I pathway of antigen processing and presentation. *Cell.* 54:777–785.
28. Porgador, A., J.W. Yewdell, Y. Deng, J.R. Bennink, and R.N. Germain. 1997. Localization, quantitation, and in situ detection of specific peptide-MHC class I complexes using a monoclonal antibody. *Immunity*. 6:715–726.
29. Stoltze, L., M. Schirle, G. Schwarz, C. Schroter, M.W. Thompson, L.B. Hersh, H. Kalbacher, S. Stevanovic, H.G. Rammensee, and H. Schild. 2000. Two new proteases in the MHC class I processing pathway. *Nat. Immunol.* 1:413–418.
30. Craiu, A., T. Akopian, A. Goldberg, and K.L. Rock. 1997. Two distinct proteolytic processes in the generation of a major histocompatibility complex class I-presented peptide. *Proc. Natl. Acad. Sci. USA.* 94:10850–10855.
31. Binder, R.J., N.E. Blachere, and P.K. Srivastava. 2001. Heat shock protein-chaperoned peptides but not free peptides introduced into the cytosol are presented efficiently by major histocompatibility complex I molecules. *J. Biol. Chem.* 276: 17163–17171.
32. Goasduff, T., and A.I. Cederbaum. 2000. CYP2E1 degradation by in vitro reconstituted systems: role of the molecular chaperone hsp90. *Arch. Biochem. Biophys.* 379:321–330.
33. Brooks, P., G. Fuertes, R.Z. Murray, S. Bose, E. Knecht, M.C. Rechsteiner, K.B. Hendil, K. Tanaka, J. Dyson, and A.J. Rivett. 2000. Subcellular localization of proteasomes and their regulatory complexes in mammalian cells. *Biochem. J.* 346:155–161.
34. Verma, R., S. Chen, R. Feldman, D. Schieltz, J. Yates, J. Dohmen, and R.J. Deshaies. 2000. Proteasomal proteomics: identification of nucleotide-sensitive proteasome-interacting proteins by mass spectrometric analysis of affinity-purified proteasomes. *Mol. Biol. Cell.* 11:3425–3439.